Defect State Analysis in Ion-Irradiated Amorphous-Silicon Heterojunctions by HAXPES

Min-I Lee, Alice Defresne, Olivier Plantevin, Denis Céolin, Jean-Pascal Rueff, Pere Roca I Cabarrocas, Antonio Tejeda

Defect state analysis in ion-irradiated amorphous-silicon heterojunctions by HAXPES

Min-I Lee,[1] Alice Defresne,[2] Oliver Plantevin,[2] Denis Ceolin,[3] Jean-Pascal Rueff,[3,4] Pere Roca i Cabarrocas,[5] and Antonio Tejeda[1,3,*]

[1] *Laboratoire de Physique des Solides, CNRS, Univ. Paris-Sud, Université Paris-Saclay, 91405 Orsay, France*

[2] *Centre de Sciences Nucléaires et de Sciences de la Matière (UMR 8609), CNRS-IN2P3-Université Paris-Sud, Université Paris-Saclay, Bat. 104-108, 91405 Orsay Campus, France*

[3] *Synchrotron SOLEIL, L'Orme des Merisiers, BP 48, Saint-Aubin, 91192 Gif-sur-Yvette Cedex, France*

[4] *Sorbonne Université, CNRS, Laboratoire de Chimie Physique -Matière et Rayonnement, F-75252 Paris, France*

[5] *Laboratoire de Physique des Interfaces et des Couches Minces (UMR 7647), CNRS-Ecole Polytechnique, Route de Saclay, 91128 Palaiseau, France*

The efficiency in HIT (Heterojunction with Intrinsic Thin film) solar cells strongly depends on the passivation of dangling bonds at the a-Si:H/c-Si interface by hydrogen, introduced in the plasma enhanced CVD process. Here in, we study controlled defects that are introduced by Ar ion irradiation. We observe by hard X-ray photoemission spectroscopy (HAXPES) that during Ar ion implantation, Si-H bonds in the a-Si:H layer are broken and become dangling bonds. We quantify the number of dangling bonds in the a-Si:H layer, and we identify the electronic states associated to them, which explains previously observed photoluminescence transitions.

I. INTRODUCTION

Since 1992, a new technology based on silicon heterostructures has partly solved the problems of high energy consumption when fabricating crystalline silicon solar cells, that was called "Heterojunction with Intrinsic Thin film (HIT)" [1]. Heterojunctions are made by combining a wide gap material such as hydrogenated amorphous silicon (a-Si:H) with an optical band gap $E_g \approx 1.7$ eV with crystalline silicon (c-Si) having a smaller band gap $E_g = 1.1$ eV. The efficiency of a-Si:H/c-Si heterojunction solar cells has reached over 26%, which is close to the theoretical conversion efficiency limit of Si solar cells ~ 29.1% [2].

One of the factors that limit the solar cell efficiency is defects. A better understanding of defects, especially at the interface between the c-Si wafer and a-Si:H could help to increase the open-circuit voltage (V_{oc}), and the short-circuit current (J_{sc}) of the heterojunction solar cells, resulting in an increase of their efficiency. Defects limit the efficiency through the additional electronic states that they generate in the band gap of a-Si:H and c-Si. At this interface, there are two kinds of defect states: mid-gap and bandtail states [3, 4]. Mid-gap states act as highly efficient recombination centers. They arise from dangling bonds [5], and are problematic for a-Si:H solar cells and other electronic devices. Bandtail states are less detrimental for the efficiency [3], and their concentration is related to the mid-gap states density [6]. They are a consequence of disordered localized electronic states appearing close to the edges of the conduction and valence bands [7].

Defects can be present on the c-Si substrates of the c-Si/a-Si:H interface and in the a-Si:H layer. In order to understand their effect and confirm their location in the stacking, we used ion implantation to generate defects. During Ar ion implantation, Si-Si and Si-H bonds in a-Si:H are broken and become dangling bonds, which is similar to the case of a-C:H, where hydrogen can be released after ion-implantation [8]. The generated dangling bonds can lead to mid-gap defect states. By controlling the energy of Ar ions, the depth of the defective region, i.e. the defect location, can be controlled [9]. Ion irradiation is therefore a convenient way to control defect formation.

Information from the defects can be obtained from photoluminescence [10]. In particular, this technique has allowed to identify defect induced states on a-Si:H heterostructures [11, 12]. Photoluminescence in different a-Si:H heterostructures shows two main peaks [9, 13]. The most intense peak at 1.1 eV corresponds to the band to band recombination in c-Si (1.1 eV). A broader and less intense peak appears at 1.2 eV, an energy smaller than the band gap of hydrogenated amorphous Si (1.7 eV) that must be associated to defect states within its gap. These states are detrimental for the solar cell efficiency due to the enhanced recombination at the interface [14]. The nature and the exact location of the states within

the gap of a-Si:H is to be identified.

In order to access the defects buried at the a-Si:H/c-Si interface, we have used hard x-ray photoemission spectroscopy (HAXPES). Different photon energies allowed us to study the defects in different regions of the a-Si:H heterojunction. We have studied the chemical environments of Si atoms, in order to quantify the number of dangling bonds and of Si-H bonds. We have also analyzed the valence band states, to observe directly the electronic states induced there by defects.

II. EXPERIMENTAL DETAILS

We have studied amorphous-silicon heterostructures consisting of undoped hydrogenated amorphous silicon (a-Si:H) and a thin layer of hydrogenated amorphous silicon carbon alloy (a-SiC:H) grown on n-type (100) single crystalline silicon wafers. The thin silicon carbon layer (3 nm) serves as a buffer layer to avoid the epitaxy of the amorphous silicon [15]. A 7 nm layer of a-Si:H is deposited on top of a-SiC:H layer. More details about the growth procedure can be found in [9].

The a-Si:H and a-SiC:H were deposited by Plasma-Enhanced Chemical Vapor Deposition (PECVD) method at 200 °C in the ARCAM reactor [16]. Once the heterostructure was produced by PECVD, defects were introduced by implanting 1keV of Ar^+ ions in a microwave source plasma reactor [13]. The Ar^+ fluence was controlled to 10^{15} $Ar.cm^{-2}$.

When dealing with buried systems, conventional photoemission does not allow to probe the core levels or the valence band. Conventional photoemission only probes the first monolayers of the material, due to the small electron escape depth upon operation with low energy photons. In order to probe the amorphous silicon heterostructure (a-Si:H/ c-Si), we used hard X-ray photoemission spectroscopy (HAXPES), a photoemission performed at high photon energies (of the order of several keV).

We measured HAXPES at GALAXIES beamline of SOLEIL synchrotron. The beamline is equipped with an in-vacuum U20 undulator delivering photons between 2.3 to 12 keV energy. The HAXPES end-station is equipped with a high energy/ high resolution electron analyzer to overcome the rapid decrease in photoionization cross section when increasing the photon energy [17, 18]. We settled a resolution of 100 meV in our experiments.

Information on depths in photoemission are obtained through the inelastic mean free path (IMFP),

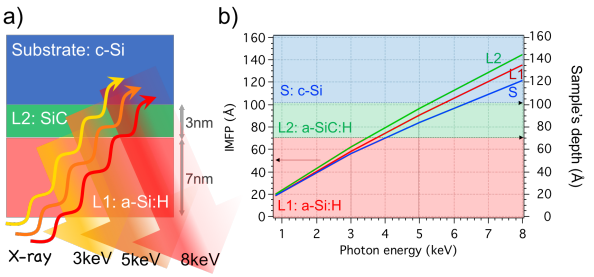

Figure 1. (a) The photoexcited electrons can be extracted from different depths of the heterojunction with different photon energies. (b) Simulation of the Inelastic Mean Free Path of electrons in Si2p for different layers (L1: a-Si:H (red), L2: a-SiC:H (green), and Substrate: c-Si (blue)) as a function of photon energy. Background colors represent the depth of each layer in the heterostructure (right axis).

related to the distance that electrons travel before suffering an inelastic collision and exciting plasmons or vibrations. The IMFP of electrons in the different core levels can be calculated by taking into account the thickness and the atomic density of each layer in the heterojunction sample.

Fig. 1 shows the IMFP calculation for electrons excited from the different layers using SESSA [19]. We have considered a thickness of 7 nm of a-Si:H (L1 = 7 nm), a bottom layer of 3 nm of a-SiC:H (L2 = 3 nm), and a 280 μm thick substrate of c-Si. The atomic densities were set to 4.90×10^{22} atom/cm^{-3}, 4.82×10^{22} atom/cm^{-3} and 4.99×10^{22} atom/cm^{-3} for L1, L2 and c-Si substrate, respectively [20–22]. Fig. 1(b) shows the IMFP of electrons from different layers as a function of photon energy. With a photon energy below 3.5 keV, most of the excited photoelectrons come from the a-Si:H layer (L1, red area). The measured electrons mainly arise from the a-Si:H layer. For studying the a-SiC:H region, a convenient energy is 5 keV, since the a-SiC:H region is reached for photons above 3.5 keV and the signal from c-Si is minimal below 5.3 keV. Finally, to reach the c-Si substrate, 8 keV photons are required. From these calculations, we selected three photon energies (3 keV, 5 keV, and 8 keV) for studying the different layers.

III. ELECTRONIC STATES INDUCED BY DEFECTS IN THE BAND STRUCTURE

In a first step, we tested our calculation of the IMFP as a function of the photon energy. We have therefore experimentally studied a 3nm thick a-Si:H

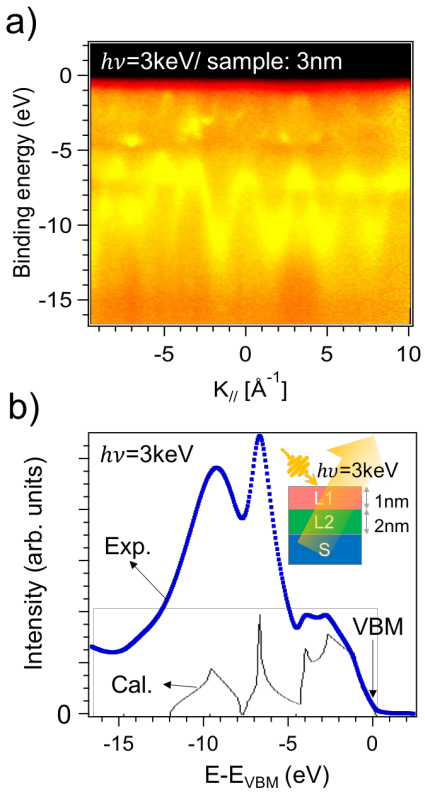

Figure 2. Electronic structure of 3 nm a-Si:H/ c-Si heterojunction sample (1 nm of a-Si:H and 2 nm of a-SiC:H) measured at 3 keV. (a) k-resolved valence band normalized to the density of states. The dispersing states from c-Si shows that we have successfully reached the buried layer of our sample. (b) Density of states along with the calculated DOS (from [24]).

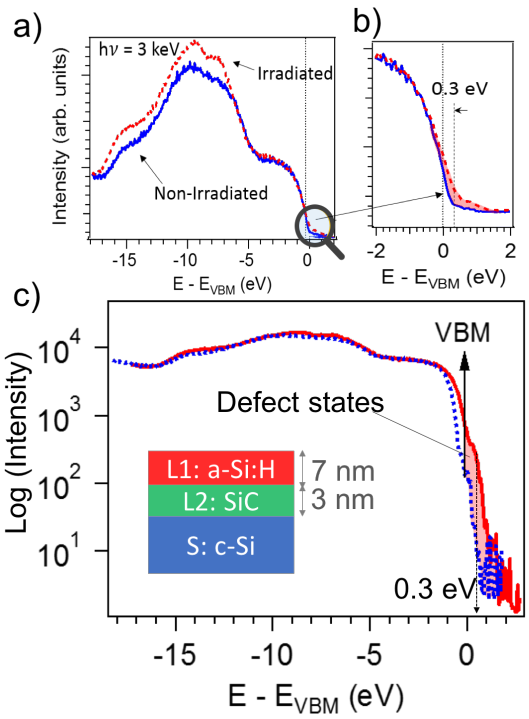

Figure 3. (a) Comparison of the experimental DOS between irradiated (red curve) and non-irradiated (blue curve) heterostructures on (d) the 10nm a-Si:H heterojunction sample. (b) Zoom at the VBM. (c) DOS in logarithmic scale. The defect states, located at 0.3 eV above valence band maximum are highlighted in pink.

heterojunction sample (1 nm a-Si:H + 2 nm SiC) on a c-Si substrate with a photon energy of 3 keV (Fig. 2). After normalizing the raw data to the density of states that contribute significantly in high photon energy photoemission [23], dispersing E(k) spectral features can be observed, indicating that we indeed reach the c-Si substrate. Our IMFP calculations are therefore correct and we can successfully reach the buried interface in our heterostructure with a correct tuning of photon energy. The experimental density of states (measured from a combination of a-Si:H and bulk c-Si) and the calculation from c-Si are plotted together in Fig. 2(b). The density of states allows to identify the valence band maximum (VBM), which will be our energy reference in the following.

To study the defect states, we focus now on a realistic heterojunction. Fig. 3 shows the integrated valence band, that emulates the DOS, from a 10 nm a-Si:H deposited on a c-Si substrate (7 nm of a-Si:H and 3 nm of SiC, see inset in Fig. 3(c)). As measured with a photon energy of 3 keV, by normalizing the spectra to the structureless high binding energy background, it can be appreciated that the spectral weight near the maximum of the valence band is higher in the irradiated heterostructures. By estimating the area difference between the irradiated and the pristine sample (integral of the pink region in Fig. 3(c)), we determine that the increase is $29 \pm 5\%$ at 3 keV , while a measurement with a photon energy of 5 keV gives an increase of $23 \pm 5\%$, the error bars being associated to the normalization process.

These gap states are located at 0.3 eV above the valence band maximum (Fig. 3(b) and (c)), and are probably associated to dangling bonds produced by irradiation. In order to determine if this atomic origin is correct, we study in the following the dangling bond variation upon irradiation.

IV. QUANTIFICATION OF DEFECTS IN THE a-Si:H LAYER

Core level spectroscopy allows to determine the different inequivalent Si atoms in the system. Moreover, core level spectroscopy is one of the rare techniques that is sensitive to H atoms. This sensitivity is obtained through the chemical shift that the bonding to a H atom induces on the core level of another element. We have therefore analyzed the Si 2p core level to identify Si-H bonds. This analysis needs the accurate decomposition of the core level into its components. Fig. 4 compares the core levels measured on non-irradiated and irradiated samples with different photon energies, all of them being normalized to the total intensity of the Si 2p core level. The spectrum on the irradiated sample at 8 keV (Fig. 4(f)) has a major contribution of a single spin-orbit splitted component which should be the one of c-Si, due to the extreme bulk sensitivity at such photon energy. The bulk component can be satisfactorily fitted with spin-splitted doublets of Voigt functions with 0.36 eV Gaussian width, 0.15 eV Lorentzian width, a spin-orbit splitting of 0.6 eV, and a branching ratio of 0.5, in agreement with [25]. After identifying the main component, residuals show the presence of other components, more explicit at other photon energies.

We have thus added the components known to be present in the a-Si:H layers and at the surface, i.e. dangling bonds, Si-H bonds and Si-O bonds. Dangling bonds appear at lower binding energies [26], so we introduced a component S1 with a chemical shift of -0.3 eV with respect to neutral silicon. We also introduced a component S2 associated to Si-H, whose binding energy is known to appear at higher binding energy than the elemental silicon [26, 27]. With these components plus an S4 component associated to Si^{4+}, usually appearing when SiO_2 is present in the system, the core level at 8 keV is satisfactorily described. By observing the Si^{4+} component (Fig. 4), it is evident that the irradiated sample is more reactive towards oxidation, because of the increase in the number of dangling bonds.

Once the spectra at 8 keV of photon energy was properly fitted, we applied the same decomposition to the other spectra by varying the intensities of the different components. For the spectra at 5 keV, with a strong contribution from the a-SiC:H layer, a new component S3 of 100.0 eV binding energy is needed for reproducing the experimental spectrum, which is precisely associated to the Si-C bonds [28]. However, a small variation can be observed in the shallower layer after the irradiation, possibly related to the carbon diffusion during the irradiation process. With these four components, all the Si 2p core levels are satisfactorily fitted. The absolute binding energy for the four components is shown in Table I.

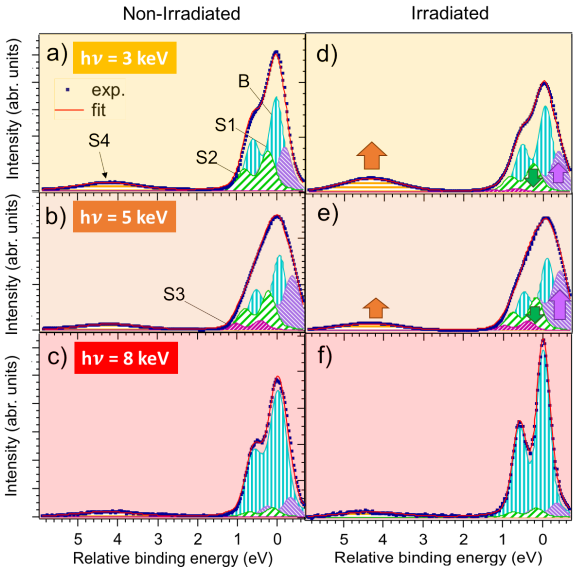

Figure 4. Si 2p core level decomposition for the non-irradiated and the irradiated heterostructures measured at photon energies of 3 keV, 5 keV and 8 keV. Five components are necessary: a bulk component which is meanly from c-Si (B), a dangling bond component (S1), a Si-H bond component (S2), a Si-C component (S3), and a Si^{4+} component that is associated to SiO_2 (S4).

	Component	Binding energy (eV)
B	Si^0	99.4±0.1
S1	dangling bond	99.1±0.1
S2	Si-H bond	99.7±0.1
S3	Si-C bond	100.0±0.1
S4	Si^{4+} bond	103.6±0.1

Table I. Absolute binding energy for B (Si^0), S1(dangling bonds), S2 (Si-H), S3 (Si-C), S4 (Si^{4+}).

The resulting decomposition is shown in Fig. 4. Component B, associated to Si^0 bulk atoms, increases at the highest probing photon energy we used (8 keV) as expected. As for the surface sensitive component S1 and S2, which are related to dangling bonds and Si-H bonds respectively, if we compare their intensities by visual inspection, we observe that the amount of dangling bonds in a-Si:H layer increases and that of Si-H bonds decreases after irradiation.

In fact, irradiation reduces the S2 intensity by 4±

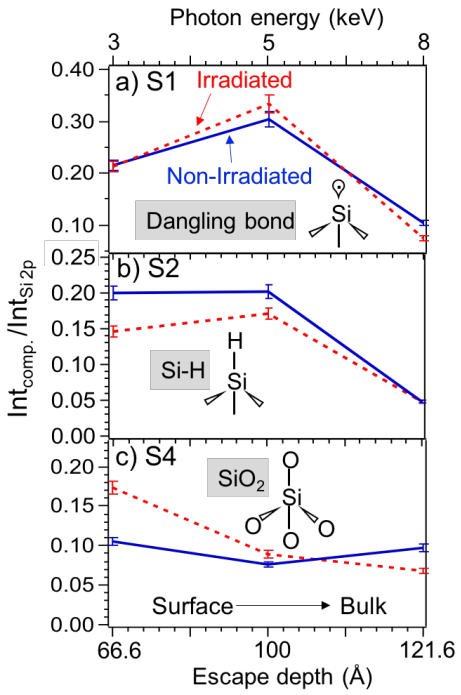

Figure 5. Intensity evolution as a function of the photon energy (top axis) and the escape depth (bottom axis) of (a) S1 component associated to dangling bonds, (b) S2 component associated to Si-H bonds, and (c) S4 component associated to silicon dioxide (Si^{4+}).

1% at both 3 keV and 5 keV (Fig. 5). Most of the intensity lost of the total area is transferred to S1 or to S4, i.e. the hydrogenated bonds are broken and become either dangling bonds or dangling bonds that interact with the oxygen when present at the surface, as seen in an increase of the S4 component at 3 keV by $7 \pm 1\%$ (Fig. 5 (c)).

We therefore observe that irradiation breaks some of the existing Si-H bonds, and increases the number of dangling bonds in the hydrogenated layers. The number of dangling bonds is correlated to the increasing intensity of the defect states at the valence band. There is indeed an increase of dangling bonds in the core level, which also relates to the intensity increase at the top of the valence band. We therefore identify the atomic origin of irradiation induced electronic states.

V. CONCLUSIONS

In conclusion, we have studied the dangling bonds formation in a-Si:H heterostructures after ion irradiation using both DOS and core level measurements with HAXPES. After the irradiation, the decrease of Si-H bonds gives raise to the increase of dangling bonds and forms the defect states. Moreover, part of those dangling bonds close to the surface has reached and forms the oxidized states of silicon. We also observe that those defect states are located at 0.3 eV above the maximum of the valence band. Since we have evidenced that those states above the maximum of the valence band cannot explain alone the 1.2 eV optical transition observed in photoluminescence, we infer the presence of defect states below the conduction band minimum, which could be probed by inverse photoemission spectroscopy in future experiments.

* antonio.tejeda@u-psud.fr

[1] Tanaka, M., Taguchi, M., Matsuyama, T., Sawada, T., Tsuda, S., Nakano, S., Hanafusa, H., and Kuwano, Y., "Development of new a-Si/c-Si heterojunction solar cells: ACJ-HIT (artificially constructed junction-heterojunction with intrinsic thin-layer)," *Japanese Journal of Applied Physics*, Vol. 31, No. 11R, 1992, pp. 3518.

[2] Yoshikawa, K., Kawasaki, H., Yoshida, W., Irie, T., Konishi, K., Nakano, K., Uto, T., Adachi, D., Kanematsu, M., Uzu, H., et al., "Silicon heterojunction solar cell with interdigitated back contacts for a photoconversion efficiency over 26%," *Nature Energy*, Vol. 2, 2017, pp. 17032.

[3] Stuckelberger, M., Biron, R., Wyrsch, N., Haug, F.-J., and Ballif, C., "Progress in solar cells from hydrogenated amorphous silicon," *Renewable and Sustainable Energy Reviews*, Vol. 76, 2017, pp. 1497–1523.

[4] Dalal, V., Knox, R., and Moradi, B., "Measurement of Urbach edge and midgap states in amorphous silicon pin devices," *Solar energy materials and solar cells*, Vol. 31, No. 3, 1993, pp. 349–356.

[5] Santos, I., Cazzaniga, M., Onida, G., and Colombo, L., "Atomistic study of the structural and electronic properties of a-Si: H/c-Si interfaces," *Journal of Physics: Condensed Matter*, Vol. 26, No. 9, 2014, pp. 095001.

[6] Stutzmann, M., "Weak bond-dangling bond conversion in amorphous silicon," *Philosophical Magazine B*, Vol. 56, No. 1, 1987, pp. 63–70.

[7] Hernandez-Como, N. and Morales-Acevedo, A., "Simulation of hetero-junction silicon solar cells with AMPS-1D," *Solar Energy Materials and Solar Cells*, Vol. 94, No. 1, 2010, pp. 62–67.

[8] Adel, M., Amir, O., Kalish, R., and Feldman, L., "Ion-beam-induced hydrogen release from a-C: H: A bulk molecular recombination model," *Journal of Applied Physics*, Vol. 66, No. 7, 1989, pp. 3248–3251.

[9] Defresne, A., Plantevin, O., Sobkowicz, I., Bourçois, J., and Roca i Cabarrocas, P., "Interface defects in

a-Si: H/c-Si heterojunction solar cells," *Nuclear Instruments and Methods in Physics Research Section B: Beam Interactions with Materials and Atoms*, Vol. 365, 2015, pp. 133–136.

[10] Dunstan, D. and Boulitrop, F., "Photoluminescence in hydrogenated amorphous silicon," *Physical Review B*, Vol. 30, No. 10, 1984, pp. 5945.

[11] Nguyen, H. T., Rougieux, F. E., Yan, D., Wan, Y., Mokkapati, S., De Nicolas, S. M., Seif, J. P., De Wolf, S., and Macdonald, D., "Characterizing amorphous silicon, silicon nitride, and diffused layers in crystalline silicon solar cells using microphotoluminescence spectroscopy," *Solar Energy Materials and Solar Cells*, Vol. 145, 2016, pp. 403–411.

[12] Street, R. and Biegelsen, D., "Luminescence and ESR studies of defects in hydrogenated amorphous silicon," *Solid State Communications*, Vol. 33, No. 12, 1980, pp. 1159–1162.

[13] Plantevin, O., Defresne, A., and Roca i Cabarrocas, P., "Suppression of the thermal quenching of photoluminescence in irradiated silicon heterojunction solar cells," *physica status solidi (a)*, Vol. 213, No. 7, 2016, pp. 1964–1968.

[14] Wang, F., Gao, Y., Pang, Z., Yang, L., and Yang, J., "Insights into the role of the interface defects density and the bandgap of the back surface field for efficient p-type silicon heterojunction solar cells," *RSC Advances*, Vol. 7, No. 43, 2017, pp. 26776–26782.

[15] Martın, I., Vetter, M., Orpella, A., Puigdollers, J., Cuevas, A., and Alcubilla, R., "Surface passivation of p-type crystalline Si by plasma enhanced chemical vapor deposited amorphous SiC x: H films," *Applied Physics Letters*, Vol. 79, No. 14, 2001, pp. 2199–2201.

[16] Roca i Cabarrocas, P., Chévrier, J., Huc, J., Lloret, A., Parey, J., and Schmitt, J., "A fully automated hot-wall multiplasma-monochamber reactor for thin film deposition," *Journal of Vacuum Science & Technology A: Vacuum, Surfaces, and Films*, Vol. 9, No. 4, 1991, pp. 2331–2341.

[17] Scofield, J. H., "Theoretical photoionization cross sections from 1 to 1500 keV." Tech. rep., California Univ., Livermore. Lawrence Livermore Lab., 1973.

[18] Yeh, J. and Lindau, I., "Atomic subshell photoionization cross sections and asymmetry parameters: $1< Z< 103$," *Atomic data and nuclear data tables*, Vol. 32, No. 1, 1985, pp. 1–155.

[19] Werner, W. S., Smekal, W., and Powell, C. J., "NIST Database for the Simulation of Electron Spectra for Surface Analysis (SESSA)," *Version 1.3, Standard Reference Program Database 100, US Department of Commerce*, National Institute of Standards and Technology Gaithersburg, MD, 2011.

[20] Custer, J., Thompson, M. O., Jacobson, D., Poate, J., Roorda, S., Sinke, W., and Spaepen, F., "Density of amorphous Si," *Applied physics letters*, Vol. 64, No. 4, 1994, pp. 437–439.

[21] Harris, G. L., *Properties of silicon carbide*, No. 13, Iet, 1995.

[22] Hull, R., *Properties of crystalline silicon*, No. 20, IET, 1999.

[23] Woicik, J. C., *Hard X-ray Photoelectron Spectroscopy (HAXPES)*, Springer, 2016.

[24] Chelikowsky, J., Chadi, D., and Cohen, M. L., "Calculated valence-band densities of states and photoemission spectra of diamond and zinc-blende semiconductors," *Physical Review B*, Vol. 8, No. 6, 1973, pp. 2786.

[25] Le Lay, G., Aristov, V. Y., and Fontaine, M., "Surface core-level shifts of Si (111) 7x7," *Le Journal de Physique IV*, Vol. 4, No. C9, 1994, pp. C9–213.

[26] Redondo, A., Goddard III, W., Swarts, C., and McGill, T., "Oxidation of silicon surfaces," *Journal of Vacuum Science and Technology*, Vol. 19, No. 3, 1981, pp. 498–501.

[27] Cerofolini, G., Galati, C., and Renna, L., "Si 2p XPS spectrum of the hydrogen-terminated (100) surface of device-quality silicon," *Surface and interface analysis*, Vol. 35, No. 12, 2003, pp. 968–973.

[28] Swain, B. P. and Hwang, N. M., "Study of structural and electronic environments of hydrogenated amorphous silicon carbonitride (a-SiCN: H) films deposited by hot wire chemical vapor deposition," *Applied Surface Science*, Vol. 254, No. 17, 2008, pp. 5319–5322.